AGU ADVANCING EARTH AND SPACE SCIENCE

Geophysical Research Letters

RESEARCH LETTER
10.1029/2020GL090360

Relativistic Electron Microbursts as High-Energy Tail of Pulsating Aurora Electrons

Y. Miyoshi[1], S. Saito[2], S. Kurita[3], K. Asamura[4], K. Hosokawa[5], T. Sakanoi[6], T. Mitani[4], Y. Ogawa[7,8], S. Oyama[1,7,9], F. Tsuchiya[6], S. L. Jones[10], A. N. Jaynes[11], and J. B. Blake[12]

[1]Institute for Space-Earth Environmental Research, Nagoya University, Nagoya, Japan, [2]National Institute of Information and Communications Technology, Koganei, Japan, [3]Research Institute for Sustainable Humanosphere, Kyoto University, Uji, Japan, [4]Institute of Space and Astronautical Science, Japan Aerospace Exploration Agency, Sagamihara, Japan, [5]Graduate School of Informatics and Engineering, The University of Electro-Communications, Chofu, Japan, [6]Graduate School of Science, Tohoku University, Sendai, Japan, [7]National Institute of Polar Research, Tachikawa, Japan, [8]The Graduate University for Advanced Studies, SOKENDAI, Hayama, Japan, [9]Space Physics and Astronomy Research Unit, University of Oulu, Oulu, Finland, [10]Goddard Space Flight Center, NASA, Greenbelt, MD, USA, [11]Department of Physics and Astronomy, University of Iowa, Iowa City, IA, USA, [12]Aerospace Corporation, Los Angeles, CA, USA

Key Points:
- We demonstrate that subrelativistic/relativistic electron microbursts are the high-energy tail of pulsating aurora electrons
- Our simulation studies demonstrate that both pulsating aurora and relativistic electron microbursts originate simultaneously
- Pulsating aurora electron and relativistic electron microbursts are the same product of chorus wave-particle interactions

Correspondence to:
Y. Miyoshi,
miyoshi@isee.nagoya-u.ac.jp

Citation:
Miyoshi, Y., Saito, S., Kurita, S., Asamura, K., Hosokawa, K., Sakanoi, T., et al. (2020). Relativistic electron microbursts as high-energy tail of pulsating aurora electrons. *Geophysical Research Letters*, *47*, e2020GL090360. https://doi.org/10.1029/2020GL090360

Received 18 AUG 2020
Accepted 7 OCT 2020
Accepted article online 13 OCT 2020
Corrected 23 APR 2021

This article was corrected on 23 APR 2021. See the end of the full text for details.

Abstract In this study, by simulating the wave-particle interactions, we show that subrelativistic/relativistic electron microbursts form the high-energy tail of pulsating aurora (PsA). Whistler-mode chorus waves that propagate along the magnetic field lines at high latitudes cause precipitation bursts of electrons with a wide energy range from a few kiloelectron volts (PsA) to several megaelectron volts (relativistic microbursts). The rising tone elements of chorus waves cause individual microbursts of subrelativistic/relativistic electrons and the internal modulation of PsA with a frequency of a few hertz. The chorus bursts for a few seconds cause the microburst trains of subrelativistic/relativistic electrons and the main pulsations of PsA. Our simulation studies demonstrate that both PsA and relativistic electron microbursts originate simultaneously from pitch angle scattering by chorus wave-particle interactions along the field line.

Plain Language Summary Pulsating aurora electron and relativistic electron microbursts are precipitation bursts of electrons from the magnetosphere to the thermosphere and the mesosphere with energies ranging from a few kiloelectron volts to tens of kiloelectron volts and subrelativistic/relativistic, respectively. Our computer simulation shows that pulsating aurora electron (low energy) and relativistic electron microbursts (relativistic energy) are the same product of chorus wave-particle interactions, and relativistic electron microbursts are high-energy tail of pulsating aurora electrons. The relativistic electron microbursts contribute to significant loss of the outer belt electrons, and our results suggest that the pulsating aurora activity can be often used as a proxy of the radiation belt flux variations.

1. Introduction

Pulsating auroras (PsAs) are caused by the intermittent precipitation of electrons with energies ranging from a few kiloelectron volts to ~100 keV from the magnetosphere to the upper atmosphere (e.g., Miyoshi et al., 2010; Sandahl et al., 1980; Yau et al., 1981). Lower-band chorus (LBC) waves cause the precipitation of these electrons through pitch angle scattering (e.g., Jaynes et al., 2013; Jones et al., 2009; Kasahara et al., 2018; Lessard, 2012; Miyoshi et al., 2010; Nishimura et al., 2010, 2020). Miyoshi, Saito et al. (2015) have proposed a model to describe the relationship between the energy spectrum of the precipitating electrons in PsA and the frequency spectrum of LBC. The intermittent precipitations of energetic electrons occurring every few seconds, which are responsible for the main modulations of the PsA, are caused by the LBC bursts. The internal modulations with a frequency of a few hertz are caused by rising tone elements of LBC embedded in each LBC burst. This model has been confirmed by recent conjugate observations (Hosokawa et al., 2020; Kasahara et al., 2018; Ozaki et al., 2019) by the Arase satellite (Miyoshi

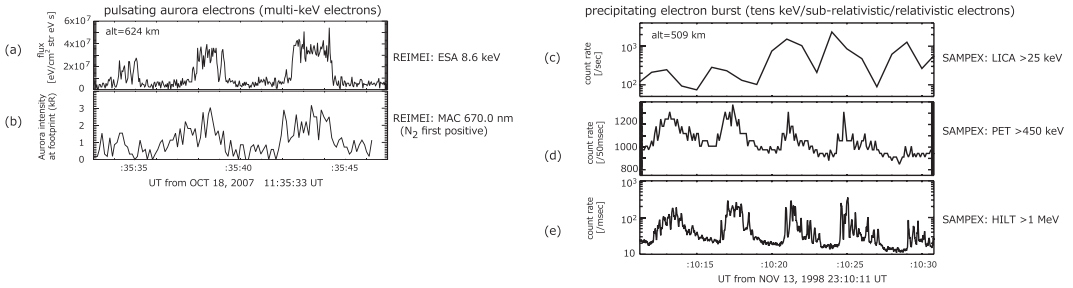

Figure 1. Variation of the precipitating electron flux with respect to time. (a) Typical variations of the precipitating electrons associated with the pulsating aurora measured by Reimei at 11:35 UTC on 18 October 2007. The corresponding energy is 8.7 keV. (b) Time variation of aurora intensity of N_2 first positive at the footprint of Reimei. Typical variations of precipitating electrons of (c) >25 keV, (d) >450 keV, and (e) >1 MeV measured by SAMPEX at 23:10 UTC on 13 November 1998. The time resolution of each data is 1 s (c), 50 ms (d), and 20 ms (e), respectively.

et al., 2018) and ground-based instruments. Miyoshi, Saito, et al. (2015) have also shown that stable precipitations from multihundred electron volts to ~ a few kiloelectron volts (e.g., Evans et al., 1987) are caused by the upper-band chorus waves.

Relativistic electron microbursts are a short-lived burst of precipitation of electrons having energies ranging from a few hundred kiloelectron volts to megaelectron volts (Blake et al., 1996; Blum & Breneman, 2020; Imhof et al., 1992; Kataoka et al., 2020; Nakamura et al., 1995; Tsurutani et al., 2013). The typical spatial scale of these microbursts is on the order of tens of kilometers (Shumko et al., 2018). The duration of the individual bursts is ~100 ms, which belongs to the same time scale as the internal modulations of the PsA and the rising tone of LBC. Anderson and Milton (1964) first reported aurora microbursts based on X-ray observations and showed that the microbursts tend to occur in "trains," where a series of 3 to 15 microbursts occur in a periodic sequence that typically would span several seconds. Recent observations have shown that these microbursts are caused by the pitch angle scattering from chorus waves (Breneman et al., 2017; Mozer et al., 2018; Shumko et al., 2020).

Figure 1a shows typical PsA electrons of 8 keV measured by the electron energy spectrum analyzers of the low-altitude Reimei satellite at 624 km altitudes (Asamura et al., 2003). The optical camera (MAC) onboard the Reimei satellite (Sakanoi et al., 2003) detected PsA with N_2 first positive (670 nm) at the footprint of the Reimei satellite as shown in Figure 1b. The main modulations with a few seconds and the subsecond internal modulations are seen in the precipitating electrons. Figure 1c shows an example of precipitating electron bursts: >30 keV electrons measured by Low-Energy Ion Composition Analyzer (Mason et al., 1993), >450 keV electrons measured by The Proton/Electron Telescope (Cook et al., 1993), and >1 MeV electrons measured by Heavy Ion Large Telescope (Klecker et al., 1993) of SAMPEX (Solar, Anomalous, and Magnetospheric Particle Explorer) at ~509 km altitudes. The time resolutions of the data are 1 s (Figure 1c), 50 ms (Figure 1d), and 20 ms (Figure 1e). The precipitations of each energy range are concurrently observed. At Figures 1d and 1e, the individual microbursts are clearly seen. Along with the individual subsecond microbursts, the trains, each of which is a series of several bursts, is seen in this observation.

Although the relationship between PsA and subrelativistic/relativistic microbursts has not been clearly understood, they are believed to originate from electron scattering by LBC. Sandahl et al. (1980) showed that ~140 keV electrons simultaneously precipitate into the ionosphere during PsA by a sounding rocket experiment. Jones et al. (2009) showed enhanced ionization at altitudes <100 km using Poker Flat Incoherent Scatter Radar observations during PsA. Miyoshi, Oyama, et al. (2015) and Oyama et al. (2017) have shown, by using the European Incoherent Scatter Radar observations, that subrelativistic and relativistic electrons precipitate into the atmosphere at altitudes <70 km in association with PsA. The microbursts of relativistic electrons are also observed above the diffuse aurora (Kurita et al., 2015). These observations suggest that subrelativistic/relativistic electron microbursts often occur simultaneously with PsA and diffuse aurora. Moreover, we expect that microburst trains are related to internal modulations embedded within the main pulsation of PsA, because both variations have the same time scales.

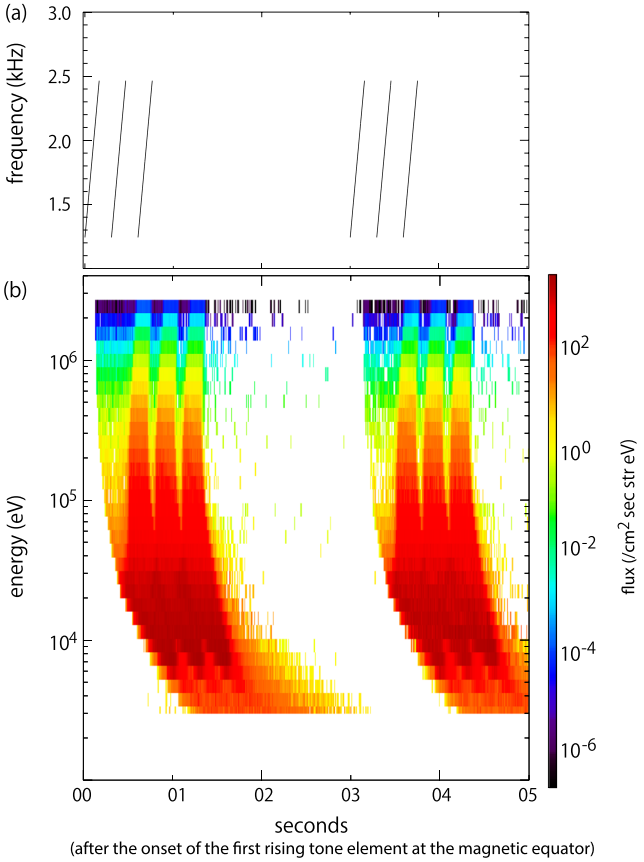

Figure 2. (a) Frequency-time diagram of the simulated chorus waves at the magnetic equator. There are two lower-band chorus bursts that include three rising tones in 5 s. (b) Variation of the precipitating electron flux with time at an altitude of 100 km calculated by the GEMSIS-RBW simulation. The color indicates the precipitating electron flux. Time indicates seconds after the onset of the first rising tone at the magnetic equator.

When LBCs propagate to high latitudes along the field lines, the resonance energy of the chorus waves becomes high because of variations of the wave dispersion relation (Horne & Thorne, 2003). Miyoshi et al. (2010) and Miyoshi, Oyama, et al. (2015) have proposed a model for wide energy precipitation of electrons having energies ranging from a few keV to several MeV by LBC propagation along the field line. Saito et al. (2012) have shown the possible energy dispersion curve for precipitating electrons by considering relativistic effects using a test-particle computer simulation. Chen et al. (2020) simulated electron microbursts induced by ducted chorus waves that propagate to the higher latitudes.

Considering these previous studies on PsA and microbursts, we propose a hypothesis that PsA and microburst originate simultaneously from the LBC wave-particle interactions, when LBC propagates to high latitudes along the field line. To confirm this hypothesis, we conducted a computer simulation for the wave-particle interactions and the resultant precipitation of wide energy electrons. We investigated the full-energy spectrum of the precipitating electrons for the first time associated with the chorus wave-particle interactions.

2. Simulations

We used the geospace environment modeling system for integrated studies-radiation belt with wave-particle interaction module test particle simulation (Saito et al., 2012), which simulates the wave-particle interaction process between LBC propagating along the field line and the bouncing electrons. The simulation estimates the temporal variation of the energy of the precipitating electrons at an altitude of 100 km. The momentum changes associated with the wave-particle interaction are given by the following equation of motion:

$$\frac{d}{dt}\mathbf{p}_e = q(\delta\mathbf{E} + \mathbf{v_e} \times (\mathbf{B} + \delta\mathbf{B})),$$

where $\mathbf{v_e} = \mathbf{p_e}/m_e\gamma$ is the electron velocity, B is the background magnetic field vector, $\mathbf{p_e}$ is the electron momentum, q is the charge of an electron, m_e is the electron rest mass, γ is the Lorentz factor, and $\boldsymbol{\delta}\mathbf{E}$ and $\boldsymbol{\delta}\mathbf{B}$ are the electric and magnetic field perturbations that satisfy the dispersion relation of the parallel propagating whistler mode wave. When electrons interact with the waves, the equation of motion is numerically solved with the time step δt during Δt, where δt is chosen to resolve the gyromotion and Δt is the time step chosen to solve the adiabatic guiding center motion. After calculation of the momentum change in Δt, the first adiabatic invariant of the electron at $t + \Delta t$ is calculated using the background magnetic field intensity at the electron position. Simultaneously with the scattering process, the electron guiding center position is advanced, in keeping with the first and second adiabatic invariants. GEMSIS-RBW (Geospace environment modeling system for integrated studies-radiation belt with wave-particle interaction module) has previously been applied for simulating PsA (Miyoshi, Oyama, et al., 2015; Miyoshi, Saito, et al., 2015), relativistic electron microbursts (Saito et al., 2012), and relativistic electron acceleration (Saito et al., 2016).

For the perturbation components, which are the same as that reported in Miyoshi, Saito, et al. (2015), LBCs are included in the model as Figure 2a. The minimum frequency and the maximum frequencies are 1.3 kHz (0.2 fc_{eq}, where fc_{eq} is the electron cyclotron frequency at the magnetic equator) and 2.5 kHz (0.4 fc_{eq}), respectively. The LBC bursts appear every 3 s, and three rising tone elements are embedded in each burst. The repeat frequency of the rising tone elements is 3 Hz, which is a typical modulation frequency of the internal modulations of PsA (Miyoshi, Oyama, et al., 2015; Royrvik & Davis, 1977). The propagation latitudes of the chorus waves are essential parameters that control the maximum energy of the resonant electrons (Miyoshi et al., 2010; Miyoshi, Oyama, et al., 2015; Saito et al., 2012). Considering the average

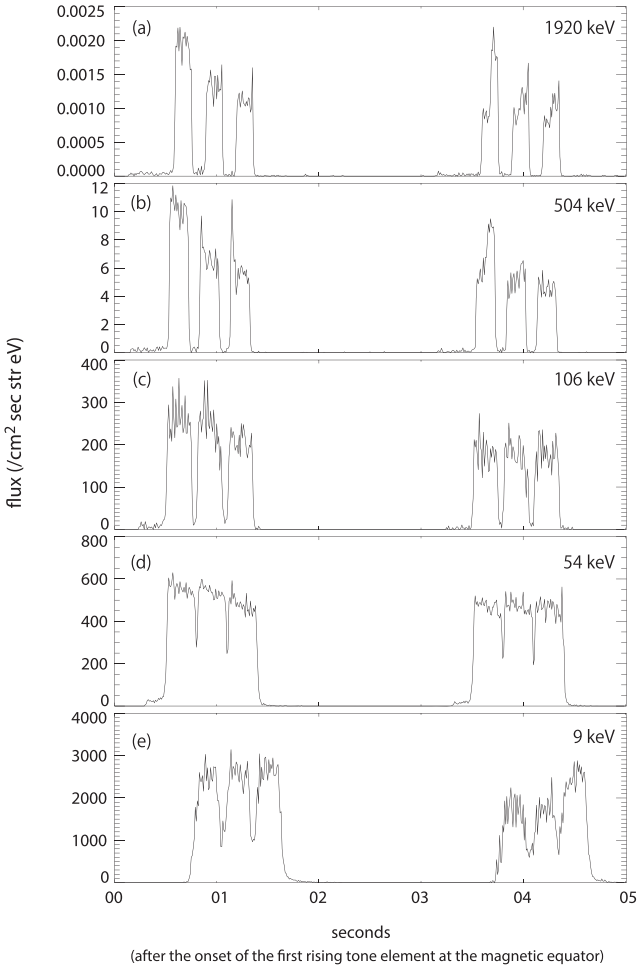

Figure 3. Temporal variation of the precipitating electrons at selected energies. Time indicates seconds after the onset of the first rising tone at the magnetic equator. (a) 1,920 keV, (b) 504 keV, (c) 106 keV, (d) 54 keV, and (e) 9 keV.

propagation latitude of chorus waves from the Cluster observations (Santolík et al., 2014), we assume that LBC can propagate to 40° magnetic latitudes along the field line.

To evaluate the flux from the test particle, we utilized the simple energy spectrum of trapped electrons in the equatorial plane defined as

$$j = j_0 \exp(-E/E_0),$$

where j is the differential electron flux, j_0 is the differential flux at the characteristic energy E_0, and E is the electron energy. In this study, j_0 is $10^7/\mathrm{cm}^2$ s str keV at $E_0 = 200$ keV. The ambient electron density n is assumed to be a constant ($n = 9/\mathrm{cm}^3$) along the field line of L-shell of 5.2. The wave amplitude of LBC is 100 pT.

3. Results

Figure 2a shows the frequency-time diagram at the magnetic equator. As we have mentioned, we put two bursts of LBC that include three rising tone elements. Figure 2b is the full energy spectrum of the precipitating electrons at the ionospheric altitudes. Two precipitations are clearly observed in association with the two LBC bursts. First, we observed the faint precipitations that show the expected energy spectrum, where the low-energy electrons arrive after the high-energy electrons at $t = 100$ ms. These electrons are not resonant with the chorus waves and are scattered into the loss cone without the resonance. Subsequently, we observed precipitations with large flux. Electrons of energy of ~30 keV are observed at $t = 500$ ms, and subsequently higher- and lower-energy electrons arrive.

Figure 3 shows variations of the flux of the precipitating electrons at different energies with respect to time. As another characteristic of the precipitating electrons, individual burst elements are clearly found at more than 100 keV. These burst element signatures with sharp enhancements and short durations are similar to the microbursts of subrelativistic/relativistic electrons. In this simulation, each rising tone element causes each precipitation burst element. Two burst trains that include three individual burst element precipitations are also seen. Since LBC bursts are assumed to appear every 3 s in this simulation as shown in Figure 2a, burst trains also appear in the same time scale as the chorus bursts.

Electrons with energies less than 100 keV do not show clearly separated burst elements because the velocity dispersion leads to broader distributions. As discussed in Miyoshi et al. (2010), different frequencies of the rising tone cause resonance of ~ keV to tens of keV electrons at different latitudes, which occur at different timings, so precipitation at the lower-energy range is continuously observed without a significant gap during the time interval of chorus bursts. Significant electron flux enhancements are seen every 3 s, and flux modulations with 3 Hz are seen in each burst, which correspond to the main modulations and internal modulations of PsA electrons (Miyoshi, Saito, et al., 2015), respectively.

The results show that the precipitations of PsA electrons with energies of tens of keV and subrelativistic/relativistic electrons are the same precipitation element. It is clearly shown that microbursts of subrelativistic/relativistic electrons are the high-energy tail of PsA electron precipitation.

4. Summary and Discussions

In this study, we have conducted the computer simulation for chorus wave-particle interactions to understand the energy spectrum variations of precipitating electrons associated with PsA. We confirm the hypothesis that chorus waves cause wide energy electron precipitations with energies ranging from a few keV (PsA) to more than several MeV (relativistic electron microbursts) simultaneously, and both PsA and the

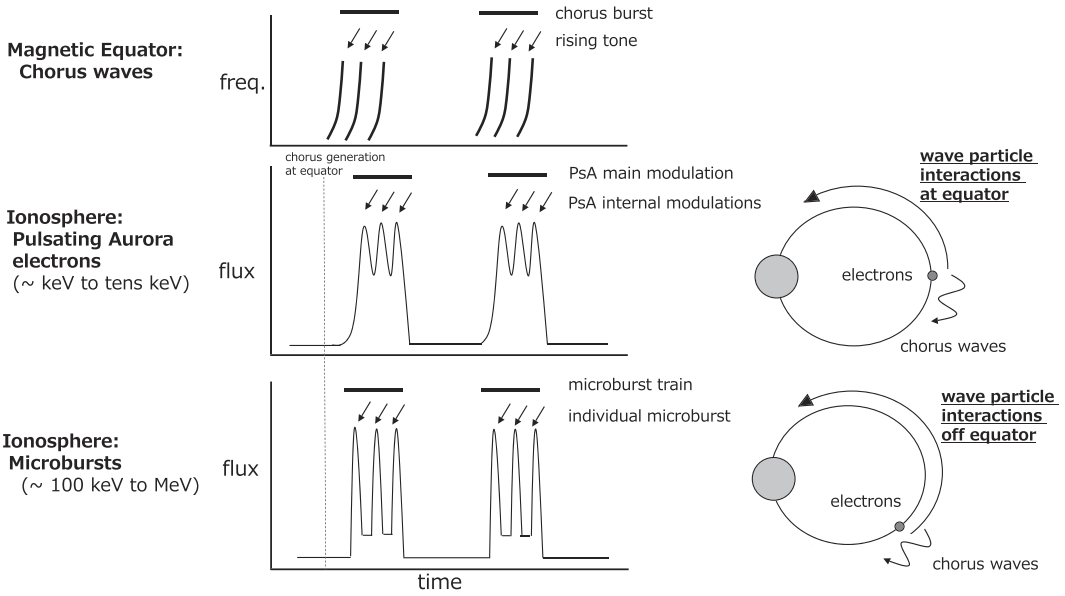

Figure 4. Schematic shows a possible connection between the temporal variations of chorus waves at the magnetic equator, PsA electrons, and relativistic electron microbursts at the ionosphere.

microbursts are the same product of chorus wave-particle interactions, and relativistic electron microbursts are high-energy tail of PsA electrons.

Time variations of precipitating electrons strongly depend on the electron energy. The main modulations and internal modulations of the PsA electrons are found to have energies from a few keV to tens of keV, which are related to the LBC frequency spectrum as shown by Miyoshi, Saito, et al. (2015). Precipitation caused by each rising tone element of LBC has a significant duration due to the velocity dispersion, and therefore, the precipitating electron flux has internal modulations within the main modulation at tens of keV. At the subrelativistic/relativistic energy range, the duration of the precipitating electrons is too short to generate the main modulation that looks the same as the PsA electrons (Lazutin, 1986; Rosenberg et al., 1981); instead, a series of individual burst precipitations make microburst trains. These variations are consistent with typical PsA and subrelativistic/relativistic microburst variations. During the bounce motion, some electrons interact with LBC several times, which sometimes cause precipitations with relatively long-duration like the main modulations, which have been observed in the past (e.g., Nakamura et al., 1995).

The higher-energy electrons resonate with the chorus waves at higher latitudes (Horne & Thorne, 2003; Miyoshi, Oyama, et al., 2015). According to the model proposed by Miyoshi et al. (2010) and Miyoshi, Oyama, et al. (2015), the higher-energy electrons travel the longer distance from the modulation region at the high latitudes to the ionospheric altitudes at the opposite hemisphere, resulting in the arrival of the higher-energy electrons after the middle-energy electrons. In contrast, electrons of the order of 10 keV arrive later because of the natural time-of-flight effects. Therefore, an energy dispersion can be found, that is, following arrival of tens of keV, lower-energy electrons and subrelativistic/relativistic electron precipitations are observed (Miyoshi et al., 2010; Saito et al., 2012).

Figure 4 shows a schematic diagram on the relationship between the temporal variations of chorus waves at the magnetic equator, PsA, and relativistic electron microbursts. Rising tone elements of LBC cause individual burst precipitations that are observed as microbursts of relativistic electrons and internal modulations of PsA electrons. The LBC bursts, which are a bundle of rising tone elements, correspond to the microburst train of relativistic electrons and the main modulations of PsA.

Differences between relativistic electron microbursts and PsA electrons are caused by the resonance energy, which depend on the wave frequency and the magnetic latitudes where the wave-particle interactions occur.

According to the resonance condition (e.g., Horne & Thorne, 2003; Miyoshi, Oyama, et al., 2015), the resonance with PsA electrons occurs around the magnetic equator, while the resonance with MeV electrons occurs at the higher-magnetic latitudes. The maximum energy of the high-energy tail of PsA is determined by the minimum frequency of LBC and the maximum propagation latitudes of LBC. The minimum energy of precipitating electrons, that is, the PsA electron, is determined by the maximum frequency of LBC and the generation latitudes of LBC that is typically considered to be around the magnetic equator. In this simulation, the maximum energy of the high-energy tail of PsA is 3 MeV, which is determined by the maximum propagation latitudes of LBC and the minimum frequency of LBC. We have assumed the uniform density along the field line. The resonance conditions also depend on the plasma density profile and field line configurations. Further simulations with different plasma density profiles and magnetic field models are important to understand characteristics of the energy dispersion.

If LBC can propagate to the higher-magnetic latitude, that is, the small ratio of plasma frequency and the electron cyclotron frequency, the energy of subrelativistic/relativistic electron microbursts becomes higher, and both PsA and subrelativistic/relativistic electron microbursts are simultaneously observed. On the other hand, if the chorus waves do not propagate to the higher-magnetic latitudes, the maximum energy of precipitating electrons becomes small, and it is expected that only tens of keV electron precipitations are found. Therefore, PsA does not always occur concurrently with subrelativistic/relativistic electron microbursts. If the radiation belt has been depleted of tens of keV electrons but still has MeV electrons, only relativistic/subrelativistic microbursts should be observed without PsA. This may happen when hiss has been able to act on the region and then the plasmasphere contracts, but no large injections of tens of keV electrons occur. Besides LBC, the electrostatic cyclotron harmonic (ECH) waves also contribute to PsA (e.g., Fukizawa et al., 2018). Since ECH mainly resonate with low-energy electrons typically less than 10 keV (e.g., Thorne et al., 2010), it is expected that PsA caused by ECH does not occur with subrelativistic/relativistic electron microbursts.

Saito et al. (2012) have shown modulation of higher frequencies than the repetition periods of the rising tone elements. They have discussed that these high-frequency modulations are due to the modulation of the pitch angle distribution near the loss cone edge through nonlinear scattering by LBC. In this simulation, we have found similar high-frequency modulations in the whole energy range as shown in Figure 3. Rapid fluctuations of electron flux, which is faster than ~10 Hz, are found at each precipitation burst, and the amplitudes of the fluctuations are different at different energies. These faster variations have been observed in the microburst (e.g., Nakamura et al., 1995) and PsA electrons (e.g., Miyoshi, Saito, et al., 2015), which may be consistent with the simulation results. Detailed analysis on the interaction processes to cause modulations will be the subject for a future study.

Recently, it has been proposed that relativistic electron precipitation causes significant ionization in the middle atmosphere and the consequent depletion of the ozone layer (e.g., Turunen et al., 2016). Our study indicates that the relativistic electron microbursts caused by the pitch angle scattering of chorus waves are the subproduct of PsA electrons, so that the continuous active PsA (e.g., Jones et al., 2013) may be a proxy for relativistic electron microbursts and the subsequent localized depletion of the ozone layer.

Blum et al. (2015) examined relativistic electron precipitations by the SAMPEX satellite, and they identified different microburst precipitations of relativistic electrons with the time scale of milliseconds and precipitation bands with longer duration (e.g., Nakamura et al., 2000). Based on different local time distributions between microbursts and precipitation bands, they suggested that chorus waves contribute to microburst of relativistic electrons in mainly postmidnight and dawn side, while electromagnetic ion cyclotron (EMIC) waves cause precipitation bands in mainly on the premidnight and dusk side. MeV electron precipitation caused by EMIC waves often occurs associated with the proton aurora at the subauroral latitudes (Miyoshi et al., 2008), and MeV electron precipitation with tens of keV proton precipitation and without tens of keV electron precipitation is caused by EMIC waves. We suggest that the proton aurora is a proxy of precipitation bands caused by EMIC waves, while PsA is a proxy of microbursts caused by the chorus waves.

Through this study, we demonstrate that subrelativistic/relativistic electron microbursts are the high-energy tail of PsA electrons. This result will be confirmed by a future sounding rocket experiment that measures wide energy electron precipitations. The LAMP (loss through auroral microburst pulsations) sounding

rocket experiment is being prepared to confirm this hypothesis by measuring the energy dispersion of the precipitating electrons of PsA and subrelativistic/relativistic electron microbursts.

Data Availability Statement

The REIMEI ESA/MAC data are opened to the public from DARTS at ISAS/JAXA (https://darts.isas.jaxa.jp/stp/reimei/). The SAMPEX HILT data are available from the SAMPEX Data Center (http://www.srl.caltech.edu/sampex/DataCenter/).

Acknowledgments
This work is supported by JSPS KAKENHI (15H05747, 16H06286, 17H00728, 20H01955, JPJSBP120194814, and 20H01959) and JSPS-CAS bilateral project.

References

Anderson, K. A., & Milton, D. W. (1964). Balloon observations of X-rays in the auroral zone: 3. High time resolution studies. *Journal of Geophysical Research*, *69*(21), 4457–4479. https://doi.org/10.1029/JZ069i021p04457

Asamura, K., Tsujita, D., Tanaka, H., Saito, Y., Mukai, T., & Hirahara, M. (2003). Auroral particle instrument onboard the INDEX satellite. *Advances in Space Research*, *32*(3), 375–378. https://doi.org/10.1016/S0273-1177(03)90275-4

Blake, J. B., Looper, M. D., Baker, D. N., Nakamura, R., Klecker, B., & Hovestadt, D. (1996). New high temporal and spatial resolution measurements by SAMPEX of the precipitation of relativistic electrons. *Advances in Space Research*, *18*(8), 171–186. https://doi.org/10.1016/0273-1177(95)00969-8

Blum, L., & Breneman, A. W. (2020). Observations of radiation belt losses due to cyclotron wave-particle interactions. In *The dynamic loss of Earth's radiation belts* (pp. 49–98). Amsterdam, Netherlands: Elsevier. https://doi.org/10.1016/B978-0-12-813371-2.0003-2

Blum, L., Li, X., & Denton, M. (2015). Rapid MeV electron precipitation as observed by SAMPEX/HILT during high-speed stream-driven storms. *Journal of Geophysical Research: Space Physics*, *120*, 3783–3794. https://doi.org/10.1002/2014JA020633

Breneman, A. W., Crew, A., Sample, J., Klumpar, D., Johnson, A., Agapitov, O., et al. (2017). Observations directly linking relativistic electron microbursts to whistler mode chorus: Van Allen Probes and FIREBIRD II. *Geophysical Research Letters*, *44*, 11,265–11,272. https://doi.org/10.1002/2017GL075001

Chen, L., Breneman, A. W., Xia, Z., & Zhang, X. -J. (2020). Modeling of bouncing electron microbursts induced by ducted chorus waves. *Geophysical Research Letters*, *47*, e2020GL089400. https://doi.org/10.1029/2020GL089400

Cook, W. R., Cummings, A. C., Cummings, J. R., Garrard, T. L., Kecman, B., Mewaldt, R. A., et al. (1993). PET: A proton/electron telescope for studies of magnetospheric, solar, and galactic particles. *IEEE Transactions on Geoscience and Remote Sensing*, *31*(3), 565–571, May 31. https://doi.org/10.1109/36.225523

Evans, D. S., Davidson, G. T., Voss, H. D., Imhof, W. L., Mobilia, J., & Chiu, Y. T. (1987). Interpretation of electron spectra in morningside pulsating aurorae. *Journal of Geophysical Research*, *92*(A11), 12,295–12,306. https://doi.org/10.1029/JA092iA11p12295

Fukizawa, M., Sakanoi, T., Miyoshi, Y., Hosokawa, K., Shiokawa, K., Katoh, Y., et al. (2018). Electrostatic electron cyclotron harmonic waves as a candidate to cause pulsating auroras. *Geophysical Research Letters*, *45*, 12,661–12,668. https://doi.org/10.1029/2018GL080145

Horne, R. B., & Thorne, R. M. (2003). Relativistic electron acceleration and precipitation during resonant interactions with whistler-mode chorus. *Geophysical Research Letters*, *30*(10), 1527. https://doi.org/10.1029/2003GL016973

Hosokawa, K., Miyoshi, Y., Ozaki, M., Oyama, S.-I., Ogawa, Y., Kurita, S., et al. (2020). Multiple time-scale beats in aurora: Precise orchestration via magnetospehric chorus waves. *Scientific Reports*, *10*, 3380. https://doi.org/10.1038/s41598-020-59642

Imhof, W. L., Voss, H. D., Mobilia, J., Datlowe, D. W., Gaines, E. E., & McGlennon, J. P. (1992). Relativistic electron microbursts. *Journal of Geophysical Research*, *97*(A9), 13,829–13,837. https://doi.org/10.1029/92JA01138

Jaynes, A. N., Lessard, M. R., Rodriguez, J. V., Donovan, E., Loto'anu, T. M., & Rychert, K. (2013). Pulsating auroral electron flux modulations in the equatorial magnetosphere. *Journal of Geophysical Research: Space Physics*, *121*, 7087–7107. https://doi.org/10.1002/2016JA022921

Jones, S., Lessard, M., Fernandes, P., Lummerzheim, D., Semeter, J., Heinselman, C., et al. (2009). PFISR and ROPA observations of pulsating aurora. *Journal of Atmospheric and Solar - Terrestrial Physics*, *71*(6-7), 708–716. https://doi.org/10.1016/j.jastp.2008.10.004

Jones, S. L., Lessard, M. R., Rychert, K., Spanswick, E., Donovan, E., & Jaynes, A. N. (2013). Persistent, widespread pulsating aurora: A case study. *Journal of Geophysical Research: Space Physics*, *118*, 2998–3006. https://doi.org/10.1002/jgra.50301

Kasahara, S., Miyoshi, Y., Yokota, S., Mitani, T., Kasahara, Y., Matsuda, S., et al. (2018). Pulsating aurora from electron scattering by chorus waves. *Nature*, *554*, 337–340. https://doi.org/10.1038/nature25505

Kataoka, R., Asaoka, Y., Torii, S., Nakahira, S., Ueno, H., Miyake, S., et al. (2020). Plasma waves causing relativistic electron precipitation event at International Space Station: Lessons from conjunction observations with Arase satellite. *Journal of Geophysical Research: Space Physics*, *125*, e2020JA027875. https://doi.org/10.1029/2020JA027875

Klecker, B., Hovestadt, D., Scholer, M., Arbinger, H., Ertl, M., Kastele, H., et al. (1993). HILT: A heavy ion large area proportional counter telescope for solar and anomalous cosmic rays. *IEEE Transactions on Geoscience and Remote Sensing*, *31*(3), 542–548. https://doi.org/10.1109/36.225520

Kurita, S., Kadokura, A., Miyoshi, Y., Morioka, A., Sato, Y., & Misawa, H. (2015). Relativistic electron precipitations in association with diffuse aurora: Conjugate observation of SAMPEX and the all sky TV camera at Syowa Station. *Geophysical Research Letters*, *42*, 4702–4708. https://doi.org/10.1002/2015GL064564

Lazutin, L. L. (1986). *X-ray emission of auroral electrons and magnetospheric dynamics* (Vol. 1986). Berlin: Springer-Verlag.

Lessard, M. (2012). A review of pulsating aurora. In A. Keiling, et al. (Eds.), *Auroral phenomenology and magnetospheric processes: Earth and other planets*, *Geophysical Monograph Series* (pp. 55–68). Washington, D. C: AGU. https://doi.org/10.1029/2011GM001187

Mason, G. M., Hamilton, D. C., Walpole, P. H., Heuerman, K. F., James, T. L., Lennard, M. H., & Mazur, J. E. (1993). LEICA: A low energy ion composition analyzer for the study of solar and magnetospheric heavy ions. *IEEE Transactions on Geoscience and Remote Sensing*, *31*(3), 549–556. https://doi.org/10.1109/36.225521

Miyoshi, Y., Katoh, Y., Nishiyama, T., Sakanoi, T., Asamura, K., & Hirahara, M. (2010). Time of flight analysis of pulsating aurora electrons, considering wave-particle interactions with propagating whistler mode waves. *Journal of Geophysical Research*, *115*, A10312. https://doi.org/10.1029/2009JA015127

Miyoshi, Y., Oyama, S., Saito, S., Kurita, S., Fujiwara, H., Kataoka, R., et al. (2015). Energetic electron precipitation associated with pulsating aurora: EISCAT and Van Allen Probes observations. *Journal of Geophysical Research: Space Physics*, *120*, 2754–2766. https://doi.org/10.1029/2014JA020690

Miyoshi, Y., Saito, S., Seki, K., Nishiyama, T., Kataoka, R., Asamura, K., et al. (2015). Relation between energy spectra of pulsating aurora electrons and frequency spectra of whistler-mode chorus waves. *Journal of Geophysical Research: Space Physics*, *120*, 7728–7736. https://doi.org/10.1002/2015JA021562

Miyoshi, Y., Sakaguchi, K., Shiokawa, K., Evans, D., Albert, J., Connors, M., & Jordanova, V. (2008). Precipitation of radiation belt electrons by EMIC waves, observed from ground and space. *Geophysical Research Letters*, *35*, L23101. https://doi.org/10.1029/2008GL035727

Miyoshi, Y., Shinohara, I., Takashima, T., Asamura, K., Higashio, N., Mitani, T., et al. (2018). Geospace exploration project ERG. *Earth, Planets and Space*, *70*, 101. https://doi.org/10.1186/s40623-018-0862-0

Mozer, F. S., Agapitov, O. V., Blake, J. B., & Vasko, I. Y. (2018). Simultaneous observations of lower band chorus emissions at the equator and microburst precipitating electrons in the ionosphere. *Geophysical Research Letters*, *45*, 511–516. https://doi.org/10.1002/2017GL076120

Nakamura, R., Bake, D. N., Blake, J. B., Kanekal, S., Klecker, B., & Hovesta, D. (1995). Relativistic electron precipitation enhancements near the outeredge of the radiation belt. *Geophysical Research Letters*, *22*(9), 1129–1132. https://doi.org/10.1029/95GL00378

Nakamura, R., Isowa, M., Kamide, Y., Baker, D. N., Blake, J. B., & Looper, M. (2000). SAMPEX observations of precipitation bursts in the outer radiation belt. *Journal of Geophysical Research*, *105*(A7), 15,875–15,885. https://doi.org/10.1029/2000JA900018

Nishimura, Y., Bortnik, J., Li, W., Thorne, R. M., Lyons, L. R., Angelopoulos, V., et al. (2010). Identifying the drive of pulsating aurora. *Science*, *330*(6000), 81–84. https://doi.org/10.1126/science.1193186

Nishimura, Y., Lessard, M. R., Katoh, Y., Miyoshi, Y., Grono, E., Partamies, N., et al. (2020). Diffuse and pulsating aurora. *Space Science Reviews*, *216*, 4. https://doi.org/10.1007/s11214-019-0629-3

Oyama, S., Kero, A., Rodger, C. J., Clilverd, M. A., Miyoshi, Y., Partamies, N., et al. (2017). Energetic electron precipitation and auroral morphology at the substorm recovery phase. *Journal of Geophysical Research: Space Physics*, *122*, 6508–6527. https://doi.org/10.1002/2016JA023484

Ozaki, M., Miyoshi, Y., Shiokawa, K., Hosokawa, K., Oyama, S. I., Kataoka, R., et al. (2019). Visualization of rapid electron precipitation via chorus element wave-particle interactions. *Nature Communications*, *10*, 257. https://doi.org/10.1038/s41467-018-07996-z

Rosenberg, T. J., Siren, J. C., Matthews, D. L., Marthinsen, K., Holtet, J. A., Egeland, A., et al. (1981). Conjugacy of electron microbursts and VLF chorus. *Journal of Geophysical Research*, *86*(A7), 5819–5832. https://doi.org/10.1029/JA086iA07p05819

Royrvik, O., & Davis, T. N. (1977). Pulsating aurora: Local and global morphology. *Journal of Geophysical Research*, *82*(29), 4720–4740. https://doi.org/10.1029/JA082i029p04720

Saito, S., Miyoshi, Y., & Seki, K. (2012). Relativistic electron microbursts associated with whistler chorus rising tone elements: GEMSIS-RBW simulations. *Journal of Geophysical Research*, *117*, A10206. https://doi.org/10.1029/2012JA018020

Saito, S., Miyoshi, Y., & Seki, K. (2016). Rapid increase in relativistic electron flux controlled by nonlinear phase trapping of whistler chorus elements. *Journal of Geophysical Research: Space Physics*, *121*, 6573–6589. https://doi.org/10.1002/2016JA022696

Sakanoi, T., Okano, S., Obuchi, Y., Kobayashi, T., Ejiri, M., Asamura, K., & Hirahara, M. (2003). Development of the multi-spectral auroral camera onboard the INDEX satellite. *Advances in Space Research*, *32*(3), 379–384. https://doi.org/10.1016/S0273-1177(3)90276-6

Sandahl, I., Eliasson, L., & Lundin, R. (1980). Rocket observations of precipitating electrons over a pulsating aurora. *Geophysical Research Letters*, *7*(5), 309–312. https://doi.org/10.1029/GL007i005p00309

Santolík, O., Macúšová, E., Kolmašová, I., Cornilleau-Wehrlin, N., & de Conchy, Y. (2014). Propagation of lower-band whistler-mode waves in the outer VanAllen belt: Systematic analysis of11 years of multi-component data from the Cluster spacecraft. *Geophysical Research Letters*, *41*, 2729–2737. https://doi.org/10.1002/2014GL059815

Shumko, M., Johnson, A. T., Sample, J. G., Griffith, B. A., Turner, D. L., O'Brien, T. P., et al. (2020). Electron microburst size distribution derived with AeroCube-6. *Journal of Geophysical Research: Space Physics*, *125*, e2019JA027651. https://doi.org/10.1029/2019JA027651

Shumko, M., Sample, J., Johnson, A., Blake, B., Crew, A., Spence, H., et al. (2018). Microburst scale size derived from multiple bounces of a microburst simultaneously observed with the Firebird-II Cubesats. *Geophysical Research Letters*, *45*, 8811–8818. https://doi.org/10.1029/2018GL078925

Thorne, R. M., Ni, B., Tao, X., Horne, R. B., & Meredith, N. P. (2010). Scattering by chorus waves as the dominant cause of diffuse auroral precipitation. *Nature*, *467*(7318), 943–946. https://doi.org/10.1038/nature09467

Tsurutani, B. T., Lakhina, G. S., & Verkhoglyadova, O. P. (2013). Energetic electron (>10 keV) microburst precipitation, ~5–15 s X-ray pulsations, chorus, and wave-particle interactions: A review. *Journal of Geophysical Research: Space Physics*, *118*, 2296–2312. https://doi.org/10.1002/jgra.50264

Turunen, E., Kero, A., Verronen, P. T., Miyoshi, Y., Oyama, S.-I., & Saito, S. (2016). Mesospheric ozone destruction by high-energy electron precipitation associated with pulsating aurora. *Journal of Geophysical Research: Atmospheres*, *121*, 11,852–11,861. https://doi.org/10.1002/2016JD025015

Yau, A. W., Whalen, B. A., & McEwen, D. J. (1981). Rocket-borne measurements of particle pulsation in pulsating aurora. *Journal of Geophysical Research*, *86*(A7), 5673–5681. https://doi.org/10.1029/JA086iA07p05673

Erratum

In the originally published version of this article, there were typos in the y-axis labels for Figure 2 and Figure 3. These have been corrected and do not affect the conclusions, and the present version may be considered the authoritative version of record.